Journal of Renewable Energies
Revue des Energies Renouvelables
journal home page : https://revue.cder.dz/index.php/rer

Research Paper

Small-signal modelling and stability analysis of island mode microgrid paralleled inverters

Ilyas Bennia[a,b], Abdelghani Harrag[a,*], Yacine Daili[a,b]

[a] Mechatronics Laboratory (LMETR), Optics and Precision Mechanics Institute, Ferhat Abbas University Sétif 1, Cite Maabouda (ex. Travaux),19000Setif, Algeria.
[b] Electrotechnics Department, Faculty of Technology, Ferhat Abbas University Sétif 1, CampusMaabouda,19000 Setif, Algeria.

A R T I C L E I N F O

Article history:
Received 12 December 2020
Accepted 03 May 2021

Keywords:
Small-signal analysis
Paralleled inverters
Island mode
Droop control
Stability analysis

A B S T R A C T

The autonomous operation mode of paralleled inverters in microgrids can be intentional or unintentional in order to ensure the continuity of supply. In this mode the voltage and frequency magnitudes are held by local controllers using droop control, this latter is generally considered to be the most adopted technic for the primary layer in a multilayer control structure due to their main feature of sharing the power equally between inverters, without needing communication infrastructure, the design of droop parameters is very crucial because a bad design can lead to the instability of the system. This paper presents a small-signal analysis for an MG composed of parallel-connected inverters in island mode and controlled using the droop method, aiming to analyze the stability by performing eigenvalues and sensitivity analysis which allows obtaining the behavior of the system, analyze the interaction between the different elements and study the influence of the droop parameters on this later which helps in the design procedure, small-signal model and Simulink block model was developed and simulated. Simulation results show a high correspondence and agreement between the model developed using Matlab Simulink-SimPowerSystem library and the developed small-signal model which confirms the validity of this later.

** Corresponding author, E-mail address: a.b.harrag@gmail.com*
Tel.: +213 796 96 61 42

ISSN: 1112-2242 / EISSN: 2716-8247

This work is licensed under a Creative Commons Attribution-ShareAlike 4.0 International License.
Based on a work at http://revue.cder.dz.

1. Introduction

In recent years, microgrids (MGs) have emerged as a new paradigm to integrate renewable energy resources and to manage power systems due to their advantages compared to the utility grids, this concept becomes a trend of the power system design, However, it presents many challenges to achieve the system reliability and resiliency, the most adapted type of control for MGs is the hierarchical control with their three layers which are responsible of different tasks to reach the target of regulating voltage and frequency, sharing power equally between inverters and managing the power flow among them and the main grid [1].

The multilayer control composed of three layers, each one is in charge of a task, the primary control carry on the voltage and frequency control with the power-sharing, the secondary layer allows the compensation of the voltage and frequency deviation, and finally the tertiary layer responsible of managing the power flow [2].

Droop control is the most adopted approach in primary control, due to their main feature of sharing the power between paralleled inverters without need for communication especially in island mode [3], the droop control provides the frequency and voltage magnitudes according to the measured active and reactive powers, however, in case of a large load transition it can be lead for losing the stability of the system, which requires a good tuning of droop parameters to deal with this problem [4].

The mathematical model based on small-signal analysis has become more and more popular for helping researchers to deal with stability and control issues in complicated systems that have multiple nonlinear components such as MGs [5], the small-signal model provides the system behavior under different circumstances and conditions, which allows obtaining the influence of controllers parameters during the design procedure [6]. The authors of [7] have proposed a grid-connected state-space model, this model takes into consideration the dynamic characteristics of the internal voltage, which is based on the swing equation of synchronous generators. Similarly, in ref [8] the authors have presented state-space modeling technics for emerging grid-connected where the converter is modeled based on the component connection method.

This paper addresses the microgrids droop control approach for paralleled inverters in both grid-connected and island modes. Moreover, a small-signal model for paralleled inverters in island mode is developed and compared with a detailed model using MATLAB Simulink software by considering two cases: in the first one, the two inverters going on in autonomous operation with the same active power references and fed a resistive load which is the standard case. In the

second one, different power set-points are adopted and no load is considered, with the same mode of operation the main difference is the first inverter fed the second one. Simulation results show a high correspondence and agreement between the detailed model and the small-signal model which confirms the validity of this later.

The rest of this paper is organized as follows: Section 2 describes the control scheme adopted in this study. In Section 3, the state-space model is developed using mathematical models; while Section 4 presents the simulation results, comparison, and discussion. Finally, Section 5 concludes the paper.

2. Microgrid control scheme

Microgrid parameters including voltage and frequency are strongly susceptible to active and reactive load changes. Frequently, there are numerous voltage source inverters (VSIs) based distributed generations (DGs) with local control, the most adopted control technic in primary control is the droop control due to the ability to adjust the MG parameters represented in the voltage and frequency while sharing the active and reactive power consumption simultaneously among parallel generation units without any need for communication infrastructure, this approach is inspired from the conventional synchronous generators control systems, in which the frequency of this later decreases when the power demand is increased[9].

The load fluctuations in an MG may cause an imbalance between generation and demand and it changes the output voltage and frequency of the VSIs according to the droop characteristics as mentioned before. If the load change is sufficiently large, the DGs may be unable to maintain the MG stability. In grid-connected mode, the control target is to reach accurate power flow regulation at the point of common coupling (PCC), it can be easily achieved using droop control or other control methods, however, the control objective in the islanded mode, is to attain precise active and reactive powers sharing and maintaining the voltage magnitude and frequency of the MG in a specific range which is reachable using the droop method. The inverter output impedance is generally considered to be inductive, thus P-ω / Q-V curves are used to determine the frequency and voltage values. Hence, the inverter can introduce the desired active and reactive power to the main grid, adjusting the output voltage and responding to linear load changes. Figure 1 shows the droop curves [10].

The droop control equations for each mode of operation (grid-connected, stand-alone modes) described as follows:

Stand-alone mode:

$$\omega = \omega^* - K_\omega P_{mes} \tag{1}$$

$$V = V^* - K_v Q_{mes} \tag{2}$$

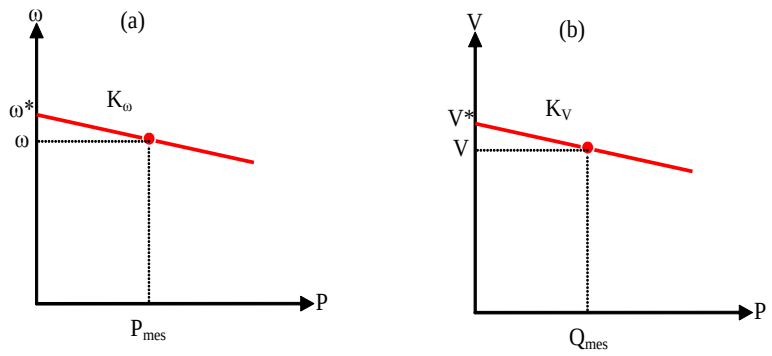

Fig. 1. Droop control characteristics:(a) P-ω curve, (b) P-V curve.

Being K_ω and K_v represents the droop control parameters and ω^*, $V*$ are the magnitude references of frequency and voltage, P_{mes}, Q_{mes} are measured and averaged active/reactive output powers, respectively.

In grid-tied mode:

$$\omega = \omega_o^* - k_\omega (P_{mes} - P^*) \tag{3}$$

$$V = V_o^* - k_v (Q_{mes} - Q^*) \tag{4}$$

Where $P*$ and $Q*$ represent the references of the powers that need to be injected, and they are set by the tertiary layer of the supervisory controller. The active P_{mes} and reactive Q_{mes} powers can be obtained by calculating it using the sensed voltage and current after this averaging them using a low pass filter (LPF) with a reduced bandwidth [11], therefore, the measured power $P_{\text{mes,}}$ and Q_{mes} are defined by:

$$P_{\text{mes}} = \frac{1}{\tau s + 1} P(s) \tag{5}$$

$$Q_{\text{mes}} = \frac{1}{\tau s + 1} Q(s) \tag{6}$$

The block diagram of the primary control for the VSI associated LCL filter is depicted in Figure 2.

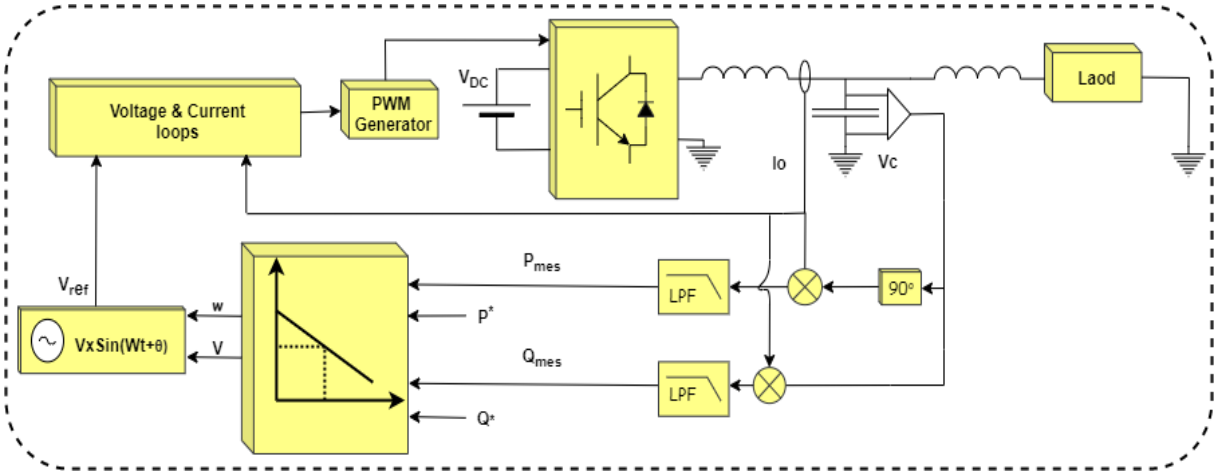

Fig. 2. Primary control diagram.

3. Small-signal model and stability analysis

To obtain the system behavior and analyze the stability using the poles of the system, a state-space model is developed, based on two paralleled single-phase inverters in autonomous operation [12], this model can be obtained using the Thevenin equivalent circuit described in Figure 3. For less complexity, the output impedance $X = \omega L_o = 2\pi(50)L_o$ have identical value for both converters and they feed a resistive load, the harmonics have not taken in consideration as they do not affect the calculated power, moreover, inner loops are not included due to their high bandwidth [13].

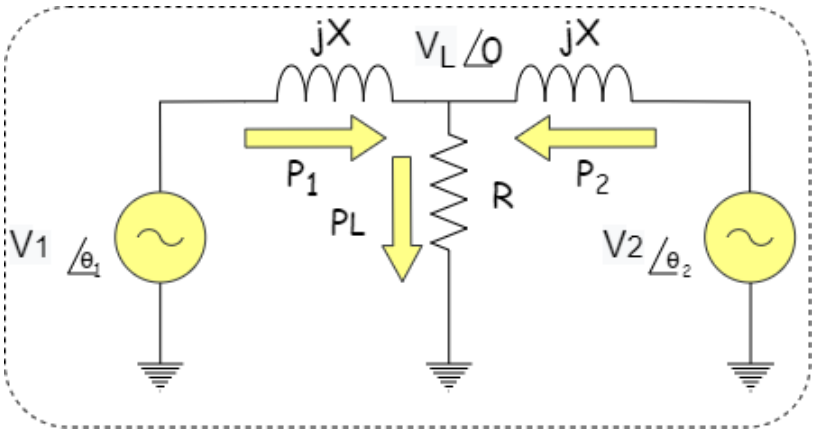

Fig. 3. Thevenin equivalent circuit of two inverters in island mode at the fundamental frequency.

The current flow from each inverter can be obtained using the following equation:

$$I_n = \frac{V_n\angle\theta_n - V_L}{X\angle 90}, n = 1,2 \tag{7}$$

Using nodes law we obtain :

$$\frac{V_L - V_1\angle\theta_1}{X\angle 90} + \frac{V_L}{R} + \frac{V_L - V_2\angle\theta_2}{X\angle 90} = 0 \tag{8}$$

From (8) the voltage load is described as :

$$V_L = \frac{R(V_1\angle\theta_1 + V_2\angle\theta_2)}{2R + X\angle 90} \tag{9}$$

The apparent power is given by

$$P_n + jQ_n = V_n I_n^*, n = 1,2 \tag{10}$$

Substituting (9) in (7) and then substituting the result in (10), the instantaneous powers can be calculated as follows :

$$P_1 = \frac{\frac{XV_1^2}{R} + 2V_1V_2\sin(\theta_1 - \theta_2) + \frac{XV_1V_2}{R}\cos(\theta_1 - \theta_2)}{4X + \frac{X^3}{R^2}} \tag{11}$$

$$Q_1 = \frac{\left(\frac{X^2}{R^2} + 2\right)V_1^2 - 2V_1V_2\cos(\theta_1 - \theta_2) + \frac{XV_1V_2}{R}\sin(\theta_1 - \theta_2)}{4X + \frac{X^3}{R^2}} \tag{12}$$

$$P_2 = \frac{\frac{XV_2^2}{R} + 2V_1V_2\sin(\theta_2 - \theta_1) + \frac{XV_1V_2}{R}\cos(\theta_2 - \theta_1)}{4X + \frac{X^3}{R^2}} \tag{13}$$

$$Q_2 = \frac{\left(\frac{X^2}{R^2} + 2\right)V_2^2 - 2V_1V_2\cos(\theta_2 - \theta_1) + \frac{XV_1V_2}{R}\sin(\theta_2 - \theta_1)}{4X + \frac{X^3}{R^2}} \tag{14}$$

Where P_1 and P_2 are the active power outputs of inverter 1 and inverter 2, Q_1 and Q_2 are the reactive power outputs of inverter 1 and inverter 2 respectively.

Considering a small perturbation around the state of equilibrium point (θ_{1eq}, θ_{2eq}, V_{1eq}, V_{2eq}) the aforementioned equations of powers can be linearized using small-signal analysis as follows :

$$\begin{aligned}\Delta P_1 &= \frac{\partial P_1}{\partial V_1}\Delta V_1 + \frac{\partial P_1}{\partial V_2}\Delta V_2 + \frac{\partial P_1}{\partial \theta_1}\Delta\theta_1 + \frac{\partial P_1}{\partial \theta_2}\Delta\theta_2 \\ &= a_1\Delta V_1 + b_1\Delta V_2 + c_1\Delta\theta_1 + d_1\Delta\theta_2\end{aligned} \tag{15}$$

$$\Delta P_2 = a_2\Delta V_1 + b_2\Delta V_2 + c_2\Delta\theta_1 + d_2\Delta\theta_2 \tag{16}$$

$$\Delta Q_1 = a_3\Delta V_1 + b_3\Delta V_2 + c_3\Delta\theta_1 + d_3\Delta\theta_2 \tag{17}$$

$$\Delta Q_1 = a_3\Delta V_1 + b_3\Delta V_2 + c_3\Delta\theta_1 + d_3\Delta\theta_2 \tag{18}$$

The Δ symbol represents a small disturbance around the state of equilibrium, the coefficient a, b,c, and d can be obtained by calculating the partial derivative correspond and the defined as follows :

$$\begin{aligned}
a_1 &= \frac{\partial P_1}{\partial V_1} = \frac{2\frac{X}{R}V_{1eq} + 2V_{2eq}\sin(\theta_{1eq}-\theta_{2eq}) + \frac{X}{R}V_{2eq}\cos(\theta_{1eq}-\theta_{2eq})}{M} \\
b_1 &= \frac{\partial P_1}{\partial V_2} = \frac{2V_{1eq}\sin(\theta_{1eq}-\theta_{2eq}) + \frac{X}{R}V_{1eq}\cos(\theta_{1eq}-\theta_{2eq})}{M} \\
c_1 &= \frac{\partial P_1}{\partial \theta_1} = \frac{2V_{1eq}V_{2eq}\cos(\theta_{1eq}-\theta_{2eq}) - \frac{X}{R}V_{1eq}V_{2eq}\sin(\theta_{1eq}-\theta_{2eq})}{M} \\
d_1 &= \frac{\partial P_1}{\partial \theta_2} = -c_1
\end{aligned} \tag{19}$$

$$\begin{aligned}
a_2 &= \frac{\partial P_2}{\partial V_1} = \frac{2V_{2eq}\sin(\theta_{2eq}-\theta_{1eq}) + \frac{X}{R}V_{2eq}\cos(\theta_{2eq}-\theta_{1eq})}{M} \\
b_2 &= \frac{\partial P_2}{\partial V_2} = \frac{2\frac{X}{R}V_{2eq} + 2V_{1eq}\sin(\theta_{2eq}-\theta_{1eq}) + \frac{X}{R}V_{1eq}\cos(\theta_{2eq}-\theta_{1eq})}{M} \\
c_2 &= \frac{\partial P_2}{\partial \theta_1} = \frac{-2V_{1eq}V_{2eq}\cos(\theta_{2eq}-\theta_{1eq}) + \frac{X}{R}V_{1eq}V_{2eq}\sin(\theta_{2eq}-\theta_{1eq})}{M} \\
d_2 &= \frac{\partial P_2}{\partial \theta_2} = -c_2
\end{aligned} \tag{20}$$

$$
\begin{aligned}
a_3 &= \frac{\partial Q_1}{\partial V_1} = \frac{2\left(\frac{X^2}{R^2}+2\right)V_{1eq} - 2V_{2eq}\cos\left(\theta_{1eq}-\theta_{2eq}\right) + \frac{X}{R}V_{2eq}\sin\left(\theta_{1eq}-\theta_{2eq}\right)}{M} \\
b_3 &= \frac{\partial Q_1}{\partial V_2} = \frac{-2V_{1eq}\cos\left(\theta_{1eq}-\theta_{2eq}\right) + \frac{X}{R}V_{1eq}\sin\left(\theta_{1eq}-\theta_{2eq}\right)}{M} \\
c_3 &= \frac{\partial Q_1}{\partial \theta_1} = \frac{2V_{1eq}V_{2eq}\sin\left(\theta_{1eq}-\theta_{2eq}\right) + \frac{X}{R}V_{1eq}V_{2eq}\cos\left(\theta_{1eq}-\theta_{2eq}\right)}{M} \\
d_3 &= \frac{\partial Q_1}{\partial \theta_2} = -c_3
\end{aligned}
\tag{21}
$$

$$
\begin{aligned}
a_4 &= \frac{\partial Q_2}{\partial V_1} = \frac{-2V_{2eq}\cos\left(\theta_{2eq}-\theta_{1eq}\right) + \frac{X}{R}V_{2eq}\sin\left(\theta_{2eq}-\theta_{1eq}\right)}{M} \\
b_4 &= \frac{\partial Q_2}{\partial V_2} = \frac{2\left(\frac{X^2}{R^2}+2\right)V_{2eq} - 2V_{1eq}\cos\left(\theta_{2eq}-\theta_{1eq}\right) + \frac{X}{R}V_{1eq}\sin\left(\theta_{2eq}-\theta_{1eq}\right)}{M} \\
c_4 &= \frac{\partial Q_2}{\partial \theta_1} = \frac{-2V_{1eq}V_{2eq}\sin\left(\theta_{2eq}-\theta_{1eq}\right) - \frac{X}{R}V_{1eq}V_{2eq}\cos\left(\theta_{2eq}-\theta_{1eq}\right)}{M} \\
d_4 &= \frac{\partial Q_2}{\partial \theta_2} = -c_4
\end{aligned}
\tag{22}
$$

Where $M = 4X + \frac{X^3}{R^2}$.

By perturbing (1) and (2) we obtain :

$$\Delta\omega_n = -k_\omega \Delta P_{\text{mesn}} \tag{23}$$

$$\Delta V_n = -k_v \Delta Q_{\text{mesn}} \tag{24}$$

Where n indicates the inverter's number. As mentioned before that the measured powers are related to the instantaneous powers as described in equations (5) and (6), and by perturbing them we obtain:

$$\Delta P_{\text{mesn}} = \frac{1}{\tau s + 1}\Delta P_n \tag{25}$$

$$\Delta Q_{\text{mesn}} = \frac{1}{\tau s + 1}\Delta Q_n \tag{26}$$

Substituting (15) in (25) and rearranging gives:

$$s\Delta P_{\text{mesn}} = \frac{1}{\tau}\left(a_n\Delta V_1 + b_n\Delta V_2 + c_n\Delta\theta_1 + d_n\Delta\theta_2\right) - \frac{1}{\tau}\Delta P_{\text{mesn}} \quad n = 1,2 \tag{27}$$

Replacing (17) in (26) gives:

$$s\Delta Q_{\text{mesn}} = \frac{1}{\tau}(a_{n+2}\Delta V_1 + b_{n+2}\Delta V_2 + c_{n+2}\Delta\theta_1 + d_{n+2}\Delta\theta_2) - \frac{1}{\tau}\Delta Q_{\text{mesn}}, n = 1,2 \tag{28}$$

The relation between the phase angle and the frequency is:

$$s\Delta\theta_n = \Delta\omega_n, \;\; n = 1,2 \tag{29}$$

After combining equations (15)-(29) and rearranging the result into a homogenous state-space equation we obtain:

$$[\mathrm{sX}_1] = [\mathrm{A}_1][\mathrm{X}_1] \tag{30}$$

Notice that [X] includes the state variables determined by:

$$[\mathrm{X}_1] = \begin{bmatrix} \Delta\theta_1 \\ \Delta\theta_2 \\ \Delta\omega_1 \\ \Delta\omega_2 \\ \Delta V_1 \\ \Delta V_2 \\ \Delta P_{\text{mes1}} \\ \Delta P_{\text{mes2}} \\ \Delta Q_{\text{mes1}} \\ \Delta Q_{\text{mes2}} \end{bmatrix}$$

and

$$[\mathrm{A1}] = \begin{bmatrix} 0 & 0 & 1 & 0 & 0 & 0 & 0 & 0 & 0 & 0 \\ 0 & 0 & 0 & 1 & 0 & 0 & 0 & 0 & 0 & 0 \\ \frac{k_\omega \cdot c_1}{\tau} & -\frac{k_\omega \cdot d_1}{\tau} & -\frac{1}{\tau} & 0 & -\frac{k_\omega \cdot a_1}{\tau} & -\frac{k_\omega b_1}{\tau} & 0 & 0 & 0 & 0 \\ -\frac{k_\omega \cdot c_2}{\tau} & -\frac{k_\omega \cdot d_2}{\tau} & 0 & -\frac{1}{\tau} & -\frac{k_\omega \cdot a_2}{\tau} & -\frac{k_\omega b_2}{\tau} & 0 & 0 & 0 & 0 \\ -\frac{k_v \cdot c_3}{\tau} & -\frac{k_v \cdot d_3}{\tau} & 0 & 0 & -\frac{(1 + k_v \cdot a_3)}{\tau} & -\frac{k_v b_3}{\tau} & 0 & 0 & 0 & 0 \\ -\frac{k_v \cdot c_4}{\tau} & -\frac{k_v \cdot d_4}{\tau} & 0 & 0 & -\frac{k_v \cdot a_4}{\tau} & -\frac{(1 + k_v b_4)}{\tau} & 0 & 0 & 0 & 0 \\ \frac{c_1}{\tau} & \frac{d_1}{\tau} & 0 & 0 & \frac{a_1}{\tau} & \frac{b_1}{\tau} & \frac{-1}{\tau} & 0 & 0 & 0 \\ \frac{c_2}{\tau} & \frac{d_2}{\tau} & 0 & 0 & \frac{a_2}{\tau} & \frac{b_2}{\tau} & 0 & \frac{-1}{\tau} & 0 & 0 \\ \frac{c_3}{\tau} & \frac{d_3}{\tau} & 0 & 0 & \frac{a_3}{\tau} & \frac{b_3}{\tau} & 0 & 0 & \frac{-1}{\tau} & 0 \\ \frac{c_4}{\tau} & \frac{d_4}{\tau} & 0 & 0 & \frac{a_4}{\tau} & \frac{b_4}{\tau} & 0 & 0 & 0 & \frac{-1}{\tau} \end{bmatrix}$$

Equation (30) defined the system for a small perturbation around the equilibrium point, the eigenvalues of matrix A_1 determine the stability and help to design the droop parameters.

4. Results and discussion

Simulation results of the developed small-signal model ($X(t) = X_{eq} + \Delta X$) are compared to the detailed model described in figure (2), which is developed using MATLAB SimpowerSystem components. The inverters are modeled as an ideal voltage source in Simulink environment with a simple time equal to 10^{-3}s, the parameters of the simulation are listed in Table (I).

Two cases are tested to confirm the small-signal model validity: i) the two inverters operate in autonomous mode with the same active power references and fed a resistive load of 20W which is the standard case; and ii) different power set-points are adopted and no load is considered, with the same mode of operation the main difference is the first inverter fed the second one. In reality, this case is not practical and it is avoided, the power set-points must be equal before starting the inverters and this is handle by the supervisory controller, it pushes the system to the margin of stability which offers a real examination for confirming the state-space model validity. Figure 4 shows the poles and zeros map of the system, it is clear that all poles and zeros are on the left side of the map with negative values which means the good stability of the system. The pzmap of the figure (4) is obtained with constants K_v=0.01 and 0.01< K_ω <1; while Figure 5 is obtained with constants 0.01< K_v <1 and K_ω=0.05.

Table I. Simulation parameters

Symbol	Description	Value	
		Case 1	Case 2
$\mathbf{P_1^*}$	Active Power reference /inverter 1	10 W	10 W
$\mathbf{P_2^*}$	Active Power reference / inverter 2	10 W	-10 W
$\mathbf{Q_1^*}$	Reactive Power reference / inverter 1	0 VAR	0 VAR
$\mathbf{Q_2^*}$	Reactive Power reference / inverter 2	0 VAR	0 VAR
$\mathbf{P_L}$	Load power	20 W	0 W
$\mathbf{L_o}$	Inverter output inductance	2500 μH	
$\mathbf{K_w}$	Frequency droop gain	$5*10^{-2}$ rad/s/W	
$\mathbf{K_v}$	Voltage droop gain	10^{-2} V/Var	
$\mathbf{f_0}$	Nominal frequency	50 Hz	
$\mathbf{V_0}$	Nominal voltage	23 Vmax	
$\boldsymbol{\tau}$	Time constant of LPF	0.1 s	

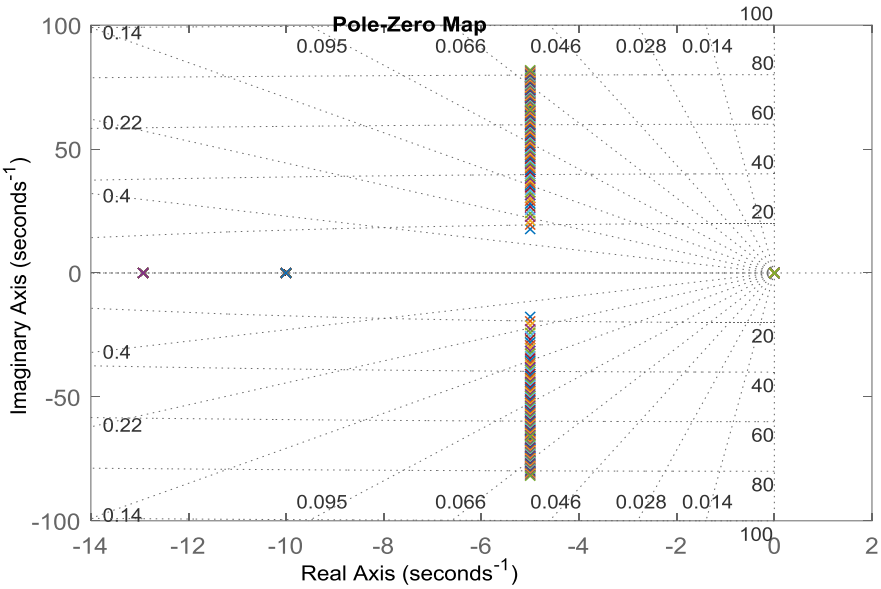

Fig. 4. Poles and zeros map of the system (Kv=0.01 and 0.01< Kω <1).

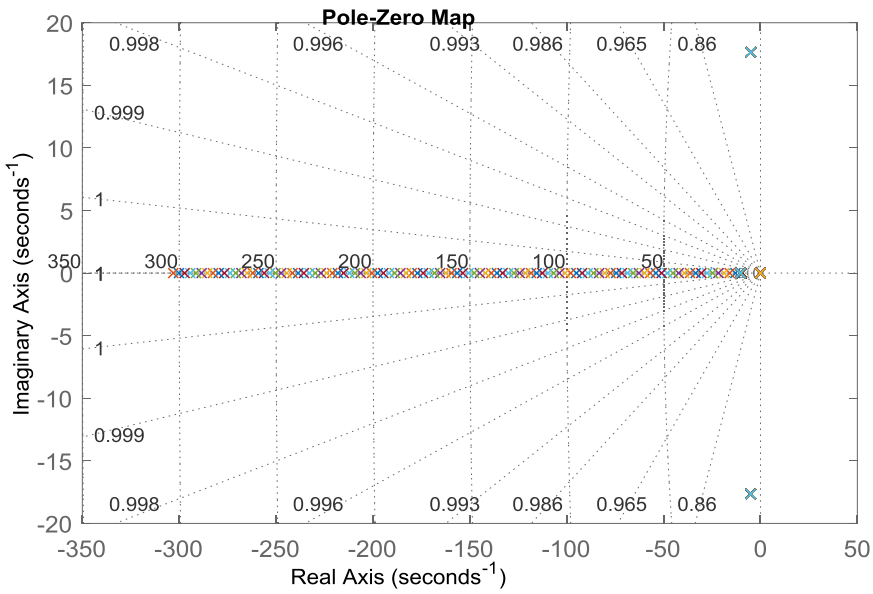

Fig. 5. Poles and zeros map of the system (0.01< Kv <1 and Kω =0.05).

Figures 6, 7, and 8 show the active powers, frequencies, and phases respectively, these figures attained from the small-signal and the full Simulink models of the two inverters under case 1 condition, it is clear there is a high matching between the small signal and the Simulink model, the two inverters provide 10 W for satisfying the load demand and sharing it equally due to the droop characteristics, with a good and fast transient dynamic, and there is a drop of frequencies due to the inherent characteristics of droop control which need to be compensated in case of sensitive loads.

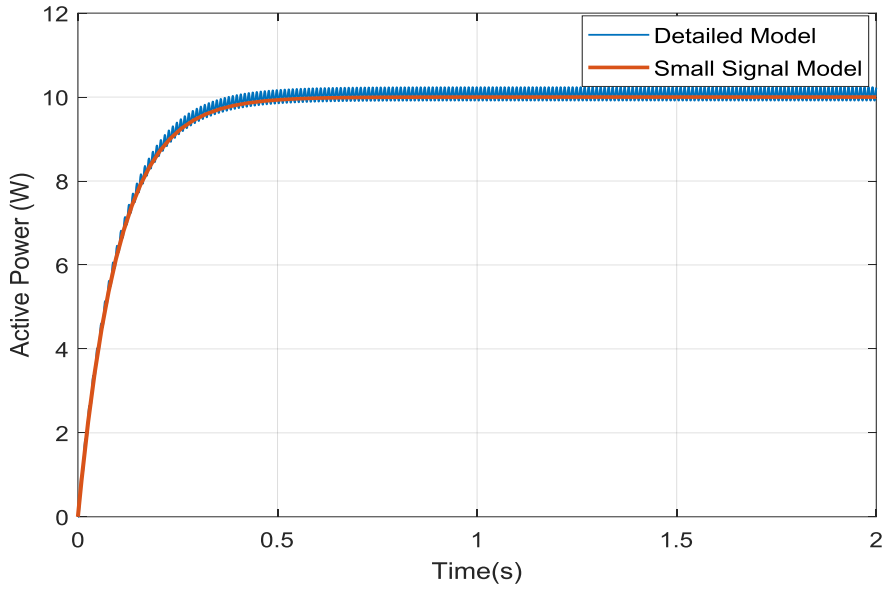

Fig. 6. Small signal and detailed model active power: Case 1

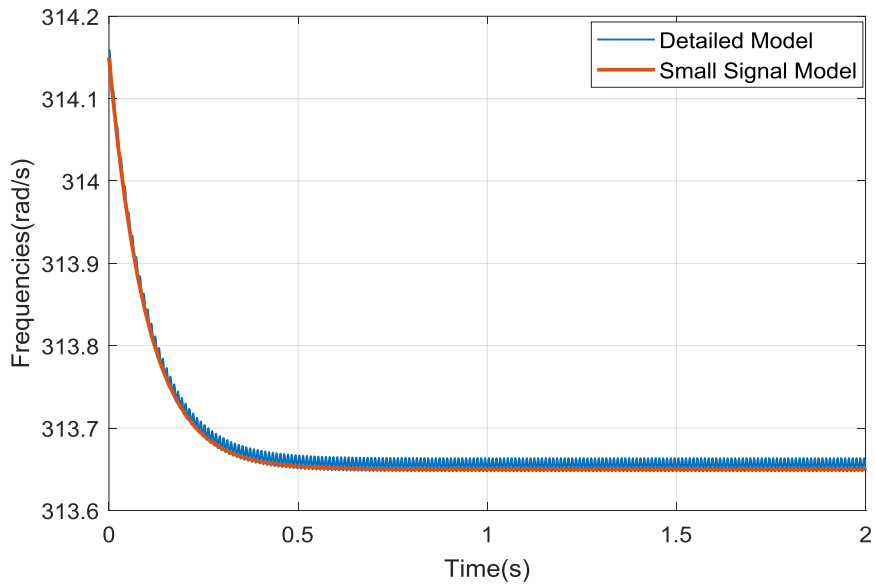

Fig. 7. Small signal and detailed model frequencies: Case 1

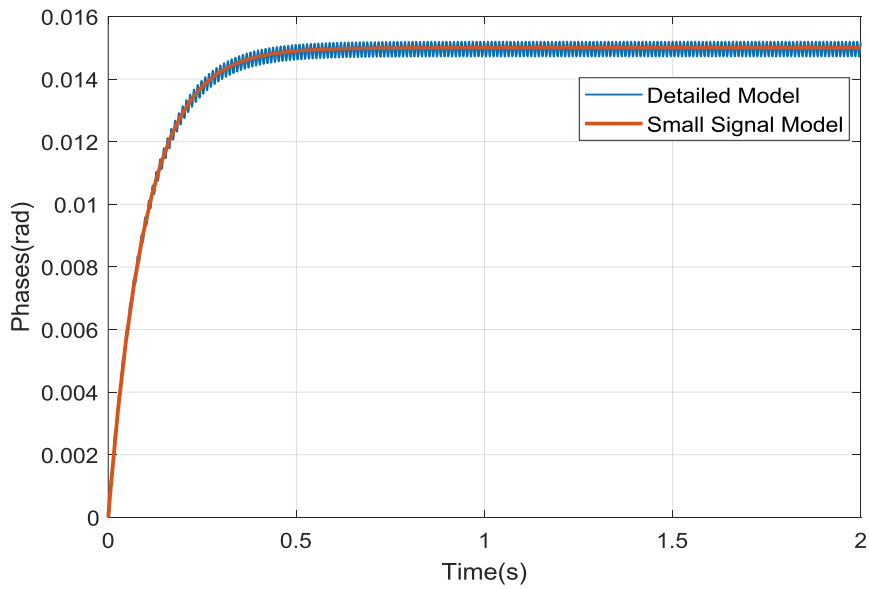

Fig. 8. Small signal and detailed model phases: Case 1

Similarly, Figures 9, 10, and 11 depict the dynamic of the active powers, frequencies, and phase angle differences, respectively, in case 2 same mode of operation without load where inverter 1 fed the inverter 2 which is an extreme case to test the stability and to push the system into the margins of stability, as can be seen, there is a complete agreement between the two models with a stable operation which confirms the good design of the system.

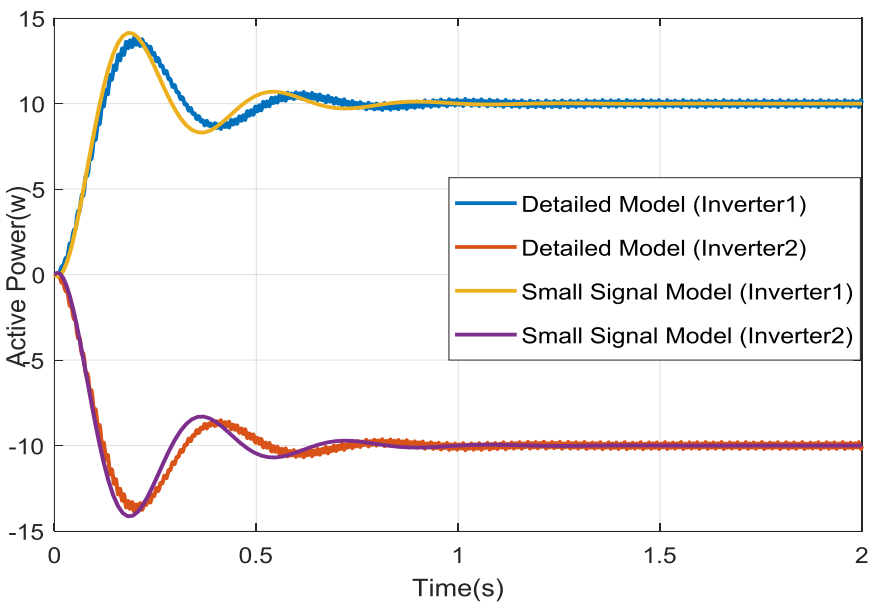

Fig. 9. Small signal and detailed model active power: Case 2

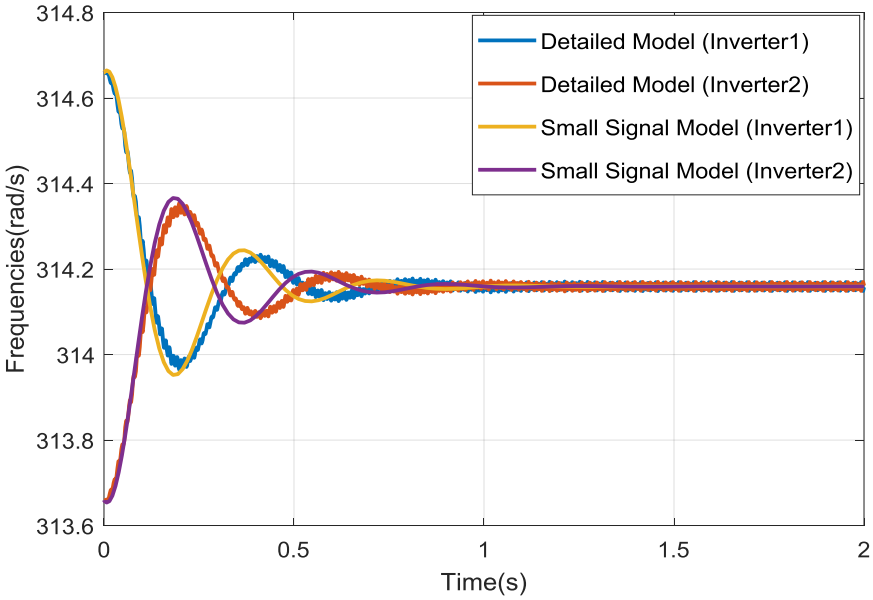

Fig. 10. Small signal and detailed model frequencies: Case 2

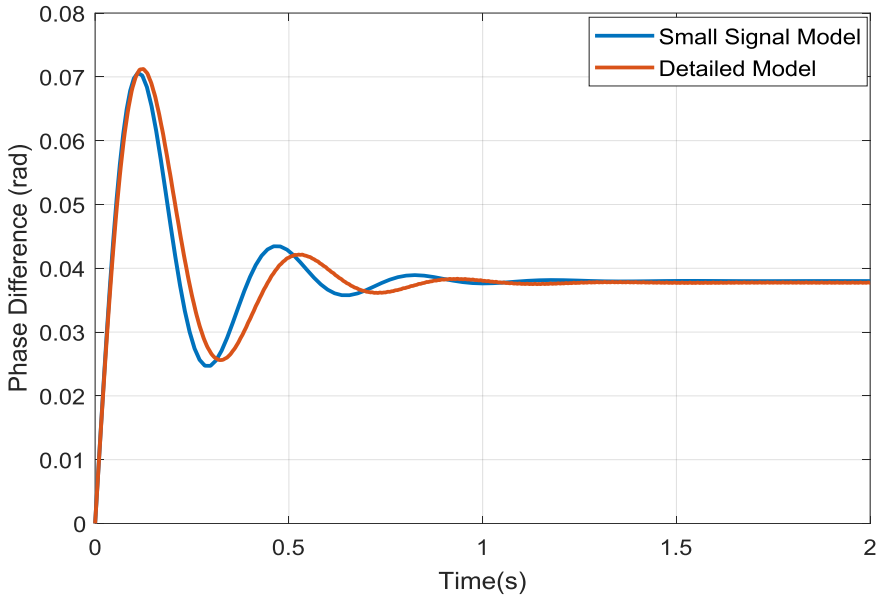

Fig. 11. Small signal and detailed model phases: Case 2

5. Conclusion

In this paper, a small-signal model for two paralleled inverters in island mode AC supply system is developed. which makes stability and performance studies easier, the developed model is simple and clear, simulation results show that the system is well represented, further a high correspondence and agreement between the detailed model and the small-signal model is

obtained which confirm the validity of this later. Based on the model and using the eigenvalue analysis method many root locus plots as a function of the system parameters can be obtained to help designers to define optimal values of droop parameters, measuring filter cutoff frequency for improved performance of the system.

6. Acknowledgements

The Algerian Ministry of Higher Education and Scientific Research via the DGRSDT supported this research (PRFU Project code: A01L07UN190120180005).

7. References

[1] Zambroni de SouzaAC & Castilla M., Microgrids Design and Implementation. Cham: Springer International Publishing, 2019.

[2] Bennia, I, Daili, Y & Harrag, A. Hierarchical Control of Paralleled Voltage Source Inverters in Islanded Single Phase Microgrids, 2020; 302-310.

[3] Daili, Y, Harrag, A. & Bennia, I. New Droop Control Technique for Reactive Power Sharing of Parallel Inverters in Islanded Microgrid, 2020; 325-10.

[4] Tayab, UB, Roslan, MAB, Hwai, LJ & Kashif, M. A review of droop control techniques for microgrid, Renew. Sustain. Energy Rev., 76, 2017; 717-10 doi: 10.1016/j.rser.2017.03.028.

[5] Paolone, M, Gaunt, T, Guillaud, X, Liserre, M, Meliopoulos, S, Monti, A, Van Cutsem, T, Vittal, V & Vournas, C. Fundamentals of power systems modelling in the presence of converter-interfaced generation, Electr. Power Syst. Res., 189, 2020: 106811.

[6] Wu, Y, Guerrero, JM, Vasquez, JC & Li, J. AC Microgrid Small-Signal Modeling: Hierarchical Control Structure Challenges and Solutions », IEEE Electrification Mag., 7(4), 2019, 81-8 doi: 10.1109/MELE.2019.2943980.

[7] Peng, Q, Yang, Y & Blaabjerg, F. State-space modeling of grid-connected power converters considering power-internal voltage characteristics, 2019; 3047-8.

[8] Mandrile, F, Musumeci, S, Carpaneto, E, Bojoi, R, Dragičević, T & Blaabjerg, F. State-Space Modeling Techniques of Emerging Grid-Connected Converters, Energies, 13(18), 2020; 4824.

[9] Guerrero, JM, Matas, J, De Vicuna, LG, Castilla, M & Miret, J. Wireless-Control Strategy for Parallel Operation of Distributed-Generation Inverters », IEEE Trans. Ind. Electron., 53(5), 2006; 1461-10 doi: 10.1109/TIE.2006.882015.

[10] Guzman, C, Cardenas, A & Agbossou, K. Hardware implementation of droop control for isolated AC microgrids. IEEE Electrical Power and Energy Conference, London, ON, Canada, oct. 2012, p. 145-150, doi: 10.1109/EPEC.2012.6474939.

[11] Guerrero, JM, De Vicuna, LG, Matas, J, Castilla, M & Miret, J. A Wireless Controller to Enhance Dynamic Performance of Parallel Inverters in Distributed Generation Systems. IEEE Trans. Power Electron., 19(5), 2004; 1205-9 doi: 10.1109/TPEL.2004.833451.

[12] Xinchun, L, Feng, F, Shanxu, D, Yong, K. & Jian, C. Modeling and stability analysis for two paralleled UPS with no control interconnection. IEEE International Electric Machines and Drives Conference, 2003. IEMDC'03., Madison, WI, USA, 2003, 3, p. 1772-1776 doi: 10.1109/IEMDC.2003.1210692.

[13] Issa, WR, Abusara, MA & Sharkh, SM. Control of Transient Power During Unintentional Islanding of Microgrids. IEEE Trans. Power Electron., 30(8), 2015; 4573-12 doi: 10.1109/TPEL.2014.2359792.